Andriy KUTSYK[1,2], Andriy LOZYNSKYY[2], Vladimir VANTSEVITCH[3], Omelian PLAKHTYNA[1,2], Lyubomyr DEMKIV[2]

UTP University of Science and Technology in Bydgoszcz (1), Lviv Polytechnic National University (2), University of Alabama at Birmingham (3)

doi:10.15199/48.2021.06.11

A Real-Time Model of Locomotion Module DTC Drive for Hardware-In-The-Loop Implementation

***Abstract**. A real-time model of AC electric motor drive for an open link locomotion module is investigated. A new numeric single-step method of average voltage on the integration step is used for the modelling of the electrical drive integrated in the locomotion model. The features of this method are the high operation performance and numerical stability. It is shown that proposed approach significantly decreases computational time, hence allowing for taking into account agile dynamics of the locomotion module when synthesizing observers or controllers*

***Streszczenie.** W niniejszej pracy przedstawiono wyniki badania modelu napędu elektrycznego AC dla modułu napędowego z otwartym łączem realizowane w czasie rzeczywistym. Do modelowania napędu elektrycznego przedstawionego w zaproponowanym modelu zastosowano nową jednostopniową metodę pomiaru średniego napięcia przy użyciu całkowania numerycznego. Cechy tej metody to wysoka wydajność i stabilność numeryczna. Wykazano, że proponowane podejście znacznie skraca czas obliczeniowy, co pozwala na uwzględnienie dynamiki modułu napędowego w budowie kontrolerów bądź systemów pomiarowych. (**Model czasu rzeczywistego modułu napędu DTC w implementacji hardware-in-the-loop**).*

Keywords: Real-time modeling, electric vehicle, asynchronous electric drive, mathematical model.
Słowa kluczowe: modelowanie czasu rzeczywistego, pojazdy elektryczne, elektryczny silnik asynchroniczny, model matematyczny.

Introduction

Hybrid modeling is an advanced method of analysis and design of complex systems, which is implemented by a combination of analog, physical and mathematical modeling. Hybrid modeling is the basis for hardware-in-the-loop technology, which integrates into a single loop the digital real-time models and physical objects [1]. This technology is widely used in various fields, including industry, aviation, aerospace and automotive for designing, synthesizing and analyzing tasks [2]. In particular, the missing elements of the real systems can be replaced by the digital model during the design stage [3]. In the power industry, the hardware-in-the-loop technology is used to synthesize and test the excitation control systems of power generators by manner of connecting the real excitation controller to the digital model of the generator block [4-6]. In paper [7] the use of real-time models for testing of control systems for vehicle's adaptive cruise control is described, and in [8] the application of such models for designing the hybrid electric vehicle's control systems is presented.

The feature of digital real-time models used in mentioned tasks is the necessity to provide continuous, stable calculation in a real time mode over a long period of time (tens of hours). The numerical integration step in such models is determined by the condition of ensuring their operation in real time mode. It depends on the processor operation performance and complexity of the model. This makes it impossible to use numerical integration methods with a variable step that are widely used to simulate stiff systems, such as electrical and power systems [1, 9]. Implicit methods of numerical integration, in particular, the trapezoidal method, have an advantage in this case. In [9] it is also noted that methods which are absolutely stable for digital systems are not always stable for hybrid systems containing an analog component. Thus, there is the problem of choosing a numerical integration method for real-time models in hybrid systems that would provide the high numeric stability and the ability to continuous, long-term calculations of stiff systems with increased value of numerical integration step (to provide the required performance).

The real-time model of electric vehicle's drive created using the author's method [10] for testing the control system of electric vehicle is proposed in present paper.

The electric vehicle's wheel actuation by advanced e-motors is one of the research and engineering directions that allows for:

- Faster torque response
- Measurable output torque through motor current
- In-wheel configuration
- Regenerative braking
- New control possibilities.

The modern technique of electrical vehicle control utilizes torque distribution between wheels by using individual electrical motors for each wheel. In this case, the direct torque control (DTC) is the most reliable motor control approach that overcomes the field-oriented control for high-performance AC motors. This method controls three-phase AC machines by estimating the flux and the motor torque by measuring the electric current and the voltage of the motor. In reference [11], the DTC was modified using a fuzzy logic approach that allowed for reducing the torque and flux ripples, which may complicate the identification process. In paper [12], a Model Reference Adaptive System observer was applied to manage the dependence of the control vector on machine parameters, and the high ripples of DTC method. A real-time implementation of the DTC together with a sliding mode controller was described in reference [13]. An FPGA-based board was used in that study to handle a significant amount of computations required for the conventional DTC implementation.

A controller that is synthesized to increase wheel mobility of the open-link locomotion also requires a model-based observer [14]. The response time of the controller heavily depends on the observer ability for quick calculations, which, in turn, depends on the accuracy of the plant model. Hence, a small reduction of the computational time can lead to a significant improvement of the controller performance. In this regard, various approaches have been investigated to reduce the computational time. One of the approaches is to simplify the model [15–17]. However, the simplification may lead to a significant loss the model fidelity.

A new approach, proposed in the present paper, allows for saving the computational time which is drastically reduced while maintaining the fidelity level of the open-link locomotion model. Obtained computational results testified the real-time applicability of the proposed approach.

Description of the method

A mathematical model of the electric drive system was developed using a numeric single-step method of average voltage on the integration step [10]. The method enables evolving a model of an electrical engineering system's power scheme as algebraic equations for branches of electrical currents. These equations are based on the equation of an electrical branch, which includes a source of e.m.f., inductance, capacitance, and active resistance:

$$\frac{1}{\Delta t}\int_{t_0}^{t_0+\Delta t}\left(u+e-u_R-u_C-u_L\right)dt=0\,, \tag{1}$$

where u is the applied voltage; u_R, u_C, u_L, e are the instantaneous values of the voltages on resistance, capacitance, inductance and e.m.f; Δt is integration step value; t_0 is the time value at the beginning of integration step.

Setting out the voltage on the active resistance and capacitor brings the two components of Eq. (1) to the following form

$$u_R=u_{R0}+\Delta u_R\,,\ u_C=u_{C0}+\Delta u_C\,, \tag{2}$$

where u_{R0}, u_{C0} are the voltages at the beginning of the numeric integration step; Δu_R, Δu_C are the voltage increments on the integration steps that are calculated as:

$$\Delta u_R=\sum_{k=1}^{\infty}\frac{d^{(k)}u_{R0}}{dt^{(k)}}\cdot\frac{(t-t_0)^k}{k!}\,,$$
$$\Delta u_C=\sum_{k=1}^{\infty}\frac{d^{(k)}u_{C0}}{dt^{(k)}}\cdot\frac{(t-t_0)^k}{k!}\,, \tag{3}$$

where $\frac{d^{(k)}u_{R0}}{dt^{(k)}}$, $\frac{d^{(k)}u_{C0}}{dt^{(k)}}$ are the k-th derivatives of the voltages on the resistance and capacitor at the beginning of the step. After taking into account the known relationships between the voltages and currents of electric branch elements, the following equation was obtained in reference [10] with the branch current, i_1, and the average voltage, U, as unknown variables at the end of the integration step:

$$U+E-u_{R0}-u_{C0}+\left(\frac{R}{m+1}+\frac{\Delta t}{C}\cdot\frac{2-(m+1)(m+2)}{2(m+1)(m+2)}+\frac{L_0}{\Delta t}\right)i_0-$$
$$-\sum_{k=1}^{m-1}\left(\frac{R\Delta t^k}{(k+1)!}\cdot\frac{m-k}{m+1}+\frac{\Delta t^{k+1}}{C(k+2)!}\cdot\frac{(m+1)(m+2)-(k+1)(k+2)}{(m+1)(m+2)}\right)\frac{d^{(k)}i_0}{dt^{(k)}}-$$
$$-\left(\frac{R}{m+1}+\frac{\Delta t}{C(m+1)(m+2)}+\frac{L_1}{\Delta t}\right)i_1=0\,, \tag{4}$$

where L_0, L_1 are the branch inductance at the beginning and end of the integration step, m is the polynomial order, which describes the current curve on the integration step (the order of the method); $U=\frac{1}{\Delta t}\int_{t_0}^{t_0+\Delta t}u dt$, $E=\frac{1}{\Delta t}\int_{t_0}^{t_0+\Delta t}e dt$ are the average voltage and voltage source values at the integration step, i_0 is the branch current value at the beginning of integration step.

A mathematical model of the system is developed using the following external vector equation, in which typical elements represented as electrical multipoles [18]

$$\vec{i}_e+\boldsymbol{G}_{se}\frac{1}{\Delta t}\int_{t_0}^{t_0+\Delta t}\vec{v}_e dt+\vec{C}_{se}=0\,, \tag{5}$$

where $\vec{v}_e$ is the vector of the multipoles' external pole potential; $\vec{i}_e$ is the currents vector of the external multipole branches; $\boldsymbol{G}_{se}$, $\vec{C}_{se}$ are the coefficient matrix and the vector of the absolute terms. Equation (5) is evolved based on Eq. (4).

As the model of an electrical engineering system is developed, the external nodes of the electrical multipoles are connected together in the nodes of the system. The connections between the average values of the multipole external potential on the integration step, $\vec{v}_e$, and the average values of the independent node potentials, $\vec{v}_c$, are described by the following equation:

$$\frac{1}{\Delta t}\int_{t_0}^{t_0+\Delta t}\vec{v}_e dt=\boldsymbol{\Pi}^T\frac{1}{\Delta t}\int_{t_0}^{t_0+\Delta t}\vec{v}_c dt\,, \tag{6}$$

where $\boldsymbol{\Pi}$ is the incidence matrix, which determines the way the external branch elements are connected to the independent nodes of the systems.

The average values of the potentials of the independent nodes on the integration step $\frac{1}{\Delta t}\int_{t_0}^{t_0+\Delta t}\vec{v}_c dt$ are obtained from the following algebraic vector equation:

$$\boldsymbol{G}_{sc}\frac{1}{\Delta t}\int_{t_0}^{t_0+\Delta t}\vec{v}_c dt+\vec{C}_{sc}=0\,, \tag{7}$$

which coefficients are defined from the formulas basing on the external vector equations (5) coefficients of all the elements that are the parts of the system, and their incidence matrices: $\boldsymbol{G}_{sc}=\sum_{j=1}^{L}\boldsymbol{\Pi}_j\boldsymbol{G}_{sej}\boldsymbol{\Pi}_j^T$, $\vec{C}_{sc}=\sum_{j=1}^{L}\boldsymbol{\Pi}_j\vec{C}_{sej}$ (L – the number of elements in the system).

The algorithm of the mathematical modelling is described below. The coefficients of Eq. (7) were calculated based on the coefficients of external vector equations (5) for all elements, which were included in the system, and their incidence matrices. Equation (7) was then used to determine the average potential values of the independent nodes on an integration step. For every structural element of the system, the average potential values of the poles on the integration step were determined from Eq. (6); the electric currents of the external branches at the end of the numeric integration step $\vec{i}_e$ were determined from Eq. (5). The variables that describe the electrical multipole and which are not the currents of the external nodes were determined from the internal equations of the electrical multipole.

When the method of average voltages on the integration step of the second and higher orders is applied, information about the derivatives of currents of the external branches is required. To calculate these derivatives, we used the principle of mathematical modelling of electromechanical systems with semiconductor converters [18].

The use of the method of average potentials on the integration step enables the algebraization of differential equations for electric current branches. In the works of [19, 20] for electric circuits with the resistance, inductance, and capacitance, the efficiency analysis was performed by comparing the abovementioned method of the second and

third order and the known methods of numeric integration, particularly Adams–Bashforth of the 4th order, Adams–Bashforth–Moulton of the 4th order, Runge–Kutt–Fehlberg of the 4th and 5th order, Dormand–Prince of the 4th order, Runge–Kutt of the 4th order, Gear of the 3rd and 4th order,the trapezium method, etc. A comparison of these methods was performed using the following metrics: the number of steps K and the computational requirements C (the product of the necessary number of steps and the number of coefficients determined at each step) on the oscillation period of current and voltages that were appropriate for obtaining the result with the prescribed accuracy. The analysis determined the best methods: the method of the average voltages on the integration step of the 3rd order (the number of steps at the oscillation period is K = 8, the computational requirement is C = 24, the mean squared errors for the current and voltage are δ_i = 0.5 % and δ_i = 0.491 %, respectively) and 2nd order (K=16, C=33, δ_i = 0.5 %, δ_i = 0.489%), and Adams–Bashforth of the 4th order (K=34, C=34, δ_i = 0.5 %, δ_i = 0.499 %), Adams–Bashforth–Moulton of the 4th order, (K=20, C=41, δ_i = 0.5 %, δ_i = 0.498 %) та Runge–Kutt–Fehlberg of the 4th order (K=7, C=42, δ_i = 0.5 %, δ_i = 0.499 %). The other abovementioned methods underperformed with higher computational requirements to achieve an appropriate accuracy. Therefore, the method of the average voltages on the integration step of the 2nd and 3rd order was selected as the optimal one since it provides the required operation performance and accuracy. It should be emphasized that the use of the 3rd order method requires a determination of the second order derivatives, which complicates the application of this method.

A computer model of an AC e-motor was created using the object-oriented approach, according to which the model of each element was presented as the object correspondent to the principles of object-oriented programming [21]. The program realization of mathematical model was formed by combining the corresponding objects of the elements. The model also included an object for connection with physical equipment, which provided information transmittance as analogous and logical signals between the computer and the physical parts of the system (if the system combines the computer models and the real physical objects).

Mathematical models

Mathematical models of the electric drive system elements were designed by applying Eq. (4) to the electrical circuit of the element, presented as multipole. The section below presents the mathematical models of an asynchronous machine and semiconductor converter.

The mathematical model of an asynchronous machine

The computational scheme of an asynchronous machine as a 12-pole (Fig. 1) contains a three-phase stator and rotor winding. Fig. 1 denotes $\left(v_{A1},v_{B1},v_{C1},v_{a1},v_{b1},v_{c1}\right)^T=\vec{v}_{am}^{\,I}$, $\left(v_{A2},v_{B2},v_{C2},v_{a2},v_{b2},v_{c2}\right)^T=\vec{v}_{am}^{\,II}$ are the poles potentials vectors, $\left(i_A,i_B,i_C,i_a,i_b,i_c\right)^T=\vec{i}_{am}$ is the vector of currents of stator and rotor winding.

As Eq. (4) for the method of the second order (m = 2) was applied to the scheme on Fig. 1, the following vector equation was obtained:

$$\vec{U}-\vec{u}_{R0}+\frac{\boldsymbol{R}_{am}}{3}\vec{i}_{am0}-\frac{\boldsymbol{R}_{am}\Delta t}{6}\frac{d\,\vec{i}_{am0}}{dt}-\frac{\boldsymbol{R}_{am}}{3}\vec{i}_{am1}-$$

$$-\frac{1}{\Delta t}\left(\vec{\psi}_{am1}-\vec{\psi}_{am0}\right)=0, \tag{8}$$

where $\vec{U}$ is the vector of the average phase voltages on the numeric integration step:

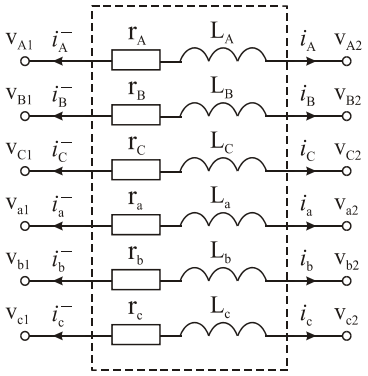

Fig.1. Computational scheme of an asynchronous machine

$$\vec{U}=\frac{1}{\Delta t}\int_{t_0}^{t_0+\Delta t}\vec{v}_{am}^{\,I}\,dt-\frac{1}{\Delta t}\int_{t_0}^{t_0+\Delta t}\vec{v}_{am}^{\,II}\,dt; \tag{9}$$

$\vec{u}_{R0}$ is the vector of the voltage drop on the active resistances of the stator and rotor winding at the beginning of the step; $\boldsymbol{R}_{am}=diag\left(R_A,R_B,R_C,R_a,R_b,R_c\right)$ is the matrix of the resistances; $\vec{i}_{am0}$, $\vec{i}_{am1}$ are the vectors of the currents at the beginning and end of the step; $\vec{\psi}_{am0}$, $\vec{\psi}_{am1}$ are the vectors of the flux linkage at the beginning and end of the step, which equal:

$$\vec{\psi}_{am0}=\boldsymbol{L}_{am0}\vec{i}_{am0}\ \text{and}\ \vec{\psi}_{am1}=\boldsymbol{L}_{am1}\vec{i}_{am1}, \tag{10}$$

where $\boldsymbol{L}_{am0}$, $\boldsymbol{L}_{am1}$ are the matrices of inductions at the beginning and end of the step; the diagonals of these matrices are the self-inductances and the other elements of these matrices are the mutual inductances, which depend on the rotor rotation angles.

Having introduced Eq. (10) and Eq. (9) in Eq. (8) and taking into the account that $\vec{u}_{R0}=\boldsymbol{R}_{am}\vec{i}_{am0}$, one can obtain:

$$\frac{1}{\Delta t}\int_{t_0}^{t_0+\Delta t}\vec{v}_{am}^{\,I}\,dt-\frac{1}{\Delta t}\int_{t_0}^{t_0+\Delta t}\vec{v}_{am}^{\,II}\,dt-\left(\frac{\boldsymbol{R}_{am}}{3}+\frac{\boldsymbol{L}_{am1}}{\Delta t}\right)\vec{i}_{am1}-$$

$$-\left(\frac{2\boldsymbol{R}_{am}}{3}-\frac{\boldsymbol{L}_{am0}}{\Delta t}\right)\vec{i}_{am0}-\frac{\boldsymbol{R}_{am}\Delta t}{6}\frac{d\,\vec{i}_{am0}}{dt}=0 \tag{11}$$

Using Eq. (11), the following equation of the asynchronous machine as a multipole can be derived:

$$\vec{i}_M+\boldsymbol{G}_M\frac{1}{\Delta t}\int_{t_0}^{t_0+\Delta t}\vec{v}_M\,dt+\vec{C}_M=0, \tag{12}$$

where $\vec{i}_M=\begin{bmatrix}-\vec{i}_{am1}\\ \vec{i}_{am1}\end{bmatrix}$ is the vector of the external branche's currents, $\vec{v}_M=\begin{bmatrix}\vec{v}_{am}^{\,I}\\ \vec{v}_{am}^{\,II}\end{bmatrix}$ is the vector of the poles potentials, coefficients matrices: $\boldsymbol{G}_M=\begin{bmatrix}\boldsymbol{R}_M^{-1} & -\boldsymbol{R}_M^{-1}\\ -\boldsymbol{R}_M^{-1} & \boldsymbol{R}_M^{-1}\end{bmatrix}$,

$\boldsymbol{R}_M=\frac{\boldsymbol{R}_{am}}{3}+\frac{\boldsymbol{L}_{am1}}{\Delta t}$,

$$\vec{C}_M = \begin{bmatrix} -\boldsymbol{R}_M^{-1}\left(\left(\frac{2\boldsymbol{R}_{am}}{3} - \frac{\boldsymbol{L}_{am0}}{\Delta t}\right)\vec{i}_{am0} + \frac{\boldsymbol{R}_{am}\Delta t}{6}\frac{d\vec{i}_{am0}}{dt}\right) \\ \boldsymbol{R}_M^{-1}\left(\left(\frac{2\boldsymbol{R}_{am}}{3} - \frac{\boldsymbol{L}_{am0}}{\Delta t}\right)\vec{i}_{am0} + \frac{\boldsymbol{R}_{am}\Delta t}{6}\frac{d\vec{i}_{am0}}{dt}\right) \end{bmatrix}.$$

Equation (12), supplemented with the equations for determination of the rotor rotation angles γ_{am}

$$\frac{d\gamma_{am}}{dt} = z_p\omega_r$$

and the velocity ω_r (the equation of the mechanical part of the electric drive), was used to calculate the asynchronous machine currents. For these calculations, the derivatives of the currents at the beginning of the step $\frac{d\vec{i}_{am0}}{dt}$ were required, which were determined based on the theory of mathematical models of the electromechanical systems with semiconductor converters [18].

The mathematical model of semiconductor converter

In this mathematical model, a semiconductor converter was considered as the scheme with the steady structure and variable parameters; every switch of the converter was represented as serially connected resistance and inductance, which took the small values as the switch was opened and the large values as the switch was closed.

The power scheme of the converter was designed by uniting the cathode and anode switch groups, which calculation circuits were identical (Fig. 2), and differed only by the direction of the current.

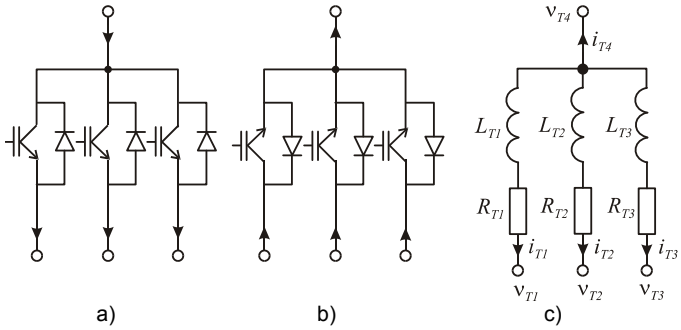

Fig.2. Power schemes of the anode (a) and cathode (b) switch groups and their calculation circuit (c)

As Eq. (4) is applied to the circuit in Fig. 2 using the 2nd order method (m = 2), the following equation can be obtained for the first branch:

$$\frac{1}{\Delta t}\int_{t_0}^{t_0+\Delta t}\vec{v}_4\,dt - \frac{1}{\Delta t}\int_{t_0}^{t_0+\Delta t}\vec{v}_1\,dt - \left(\frac{R_{T1}}{3} + \frac{L_{T1}}{\Delta t}\right)\vec{i}_{T1_1} -$$

$$-\left(\frac{2R_{T1}}{3} - \frac{L_{T1}}{\Delta t}\right)\vec{i}_{T1_0} - \frac{R_{T1}\Delta t}{6}\frac{d\vec{i}_{T1_0}}{dt} = 0 \quad (13)$$

The positive values of the current in Eq. (13) correspond to the transistor current, and the negative values correspond to the feedback diode. Having compiled the similar equations for the other branches and taking into the account $i_{T4} = -(i_{T1} + i_{T2} + i_{T3})$, the following vector equation is received:

$$\vec{i}_T + \boldsymbol{G}_T\frac{1}{\Delta t}\int_{t_0}^{t_0+\Delta t}\vec{v}_T\,dt + \vec{C}_T = 0 \quad (14)$$

where $\vec{i}_T = \left(i_{T1_1}, i_{T2_1}, i_{T3_1}, i_{T4_1}\right)^T$ is the vector of the external branches currents, $\vec{v}_T = \left(v_{T1}, v_{T2}, v_{T3}, v_{T4}\right)^T$ is the vector of poles potentials, coefficients matrices:

$$\boldsymbol{G}_T = \begin{bmatrix} R_{T1}^{*-1} & 0 & 0 & -R_{T1}^{*-1} \\ 0 & R_{T2}^{*-1} & 0 & -R_{T2}^{*-1} \\ 0 & 0 & R_{T3}^{*-1} & -R_{T3}^{*-1} \\ -R_{T1}^{*-1} & -R_{T2}^{*-1} & -R_{T3}^{*-1} & \sum_{i=1}^{3} R_{Ti}^{*-1} \end{bmatrix}, \quad (15)$$

$$R_{Ti}^{*} = \frac{R_{Ti}}{3} + \frac{L_{Ti}}{\Delta t} \ (i=1,2,3),$$

$$\vec{C}_T = \begin{bmatrix} R_{T1}^{*-1}\left(\left(\frac{2R_{T1}}{3} - \frac{L_{T1}}{\Delta t}\right)\vec{i}_{T1_0} + \frac{R_{T1}\Delta t}{6}\frac{d\vec{i}_{T1_0}}{dt}\right) \\ R_{T2}^{*-1}\left(\left(\frac{2R_{T2}}{3} - \frac{L_{T2}}{\Delta t}\right)\vec{i}_{T2_0} + \frac{R_{T2}\Delta t}{6}\frac{d\vec{i}_{T2_0}}{dt}\right) \\ R_{T3}^{*-1}\left(\left(\frac{2R_{T3}}{3} - \frac{L_{T3}}{\Delta t}\right)\vec{i}_{T3_0} + \frac{R_{T3}\Delta t}{6}\frac{d\vec{i}_{T3_0}}{dt}\right) \\ -\sum_{i=1}^{3} R_{Ti}^{*-1}\left(\left(\frac{2R_{Ti}}{3} - \frac{L_{Ti}}{\Delta t}\right)\vec{i}_{Ti_0} + \frac{R_{Ti}\Delta t}{6}\frac{d\vec{i}_{Ti_0}}{dt}\right) \end{bmatrix}.$$

The link parameters, R_T and L_T, were determined by the state of the current link switches, i.e., the transistor and feedback diode. The state of the switches was determined from the logical equations, which described the DTC transformer control system.

To calculate the currents of the switches their derivatives are necessary (in case of using the method of the second order). The introduction of inductance in the branch, which equivalents a switch, makes it possible to determine the derivative of the switch current from the electrical circuit equations arranged according to Kirchhoff's second law. The procedure for determining derivatives is described in [18].

The mathematical model of the open-link locomotion module

This study was conducted for the e-drive shown in Fig. 3, in which the e-motor is connected to the drive wheel by the means of a transmission gearbox.

The wheel dynamics is defined according to references [22, 23]. The battery is modeled using the gain factor, k_{bat}, while neglecting possible PWM oscillations that may occur under the influence of the controller. The development of the controller is outside the scope of the current paper. The nonlinearities that are present in the gearbox (i.e. frictions, hysteresis etc.) are not taken into account. Hence the gearbox is modeled as a gain factor r_v.

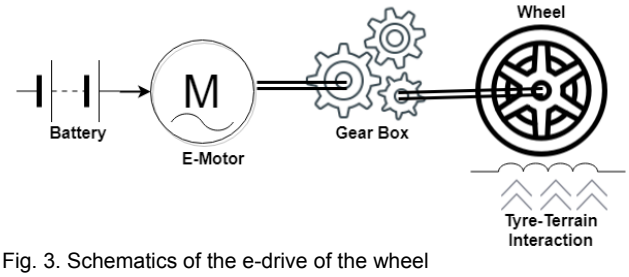

Fig. 3. Schematics of the e-drive of the wheel

The dynamical model of the wheel can be described by the following equations (see [22, 23])

$$\begin{cases} \dfrac{d\omega_m(t)}{dt} = \dfrac{1}{J_m}\left(k_t i_m(t) - r_v T_{sd}(t)\right) \\ \dfrac{dT_{sd}(t)}{dt} = k_{sh} r_v \omega_m(t) - k_{sh}\omega_w(t) \\ \dfrac{d\omega_w(t)}{dt} = \dfrac{1}{J_w(R_z)}\left(T_{sd}(t) - T_{wl}(t)\right) \\ R_z = W_w \cos\theta_n + k_{tg}(z_r - z_u) + c_{tg}(\dot{z}_r - \dot{z}_u) \\ m_s \ddot{z}_s = k_s(z_u - z_s) + c_s(\dot{z}_u - \dot{z}_s) \\ m_u \ddot{z}_u = k_{tg}(z_r - z_u) + c_{tg}(\dot{z}_r - \dot{z}_u) - k_s(z_u - z_s) - c_s(\dot{z}_u - \dot{z}_s) \end{cases}$$

where $\omega_w(t)$ is the angular velocity of wheel, J_w is the moment of inertia of the wheel which depends on the wheel normal reaction R_z, $T_{wl}(t)$ corresponds to tyre-terrain interaction which was modeler according to [24], T_{sd} is the elastic-damping torque, θ_n is the slope of the surface of motion, W_w is the static load on the wheel caused by the sprung mass and unsprung mass, k_{tg} is the tire-soil longitudinal stiffness, c_{tg} is the tire-soil damping factor, z_s, z_u are the displacement of the sprung and unsprung masses (see Fig. 4.), m_s and m_u, z_r is the change in the road height from its zero reference height k_s is the reduced stiffness of the suspension, cs is the reduced damping of the suspension, k_{sh} is the shaftelasticity.

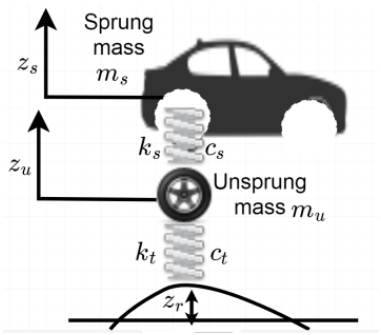

Fig. 4. Vibration model of the open-link locomotion model..

Results

The following parameters of the asynchronous transmission drive of the electric car wheel were used for the research: P = 110 kW, U = 380 V, f = 50 Hz, R_s = 0.04 Ω, R'_r = 0.04 Ω, $L_{\sigma s} = L'_{\sigma r}$ = 0.00025 H, L_m = 0.011 H, z_p = 4, J = 15 kg · m^2. The parameters for the mechanical part: m_u = 336.26 kg, m_s = 2353.8 kg, C_s = 13000 Ns/m, C_{tg} = 1740 Ns/m, J_m = 0.008 kgm^2, k_{bat} = 120 V, k_s = 2500 Nm, k_t = 0.5 Nm/A, K_s = 50000 N/m, K_{tg} = 96130 N/m, r_v = 1/9.73.

To assess the adequacy of the developed model of asynchronous electric drive with the DTC, the obtained results were compared to standard Matlab/Simulink computer simulation of analogical asynchronous electric drive with the appropriate parameters applied. The comparison is depicted in Fig. 5 for the regimes of velocity and load change. The results prove the adequacy of the developed model. For calculations, the developed model used 0.00003 s numeric integration step, and the calculations were performed in real-time when the calculated time corresponded to the real time. The calculation with the similar integration step for the Matlab/Simulink model of analogical asynchronous electric drive with the DTC was five times slower, which disabled its real-time application.

Fig. 6 illustrates computational results of the acceleration performance of the open-link locomotion module while speeding up to the maximal velocity (105 km/h), which corresponds to the rotation speed of the asynchronous drive of 700 rev/min.

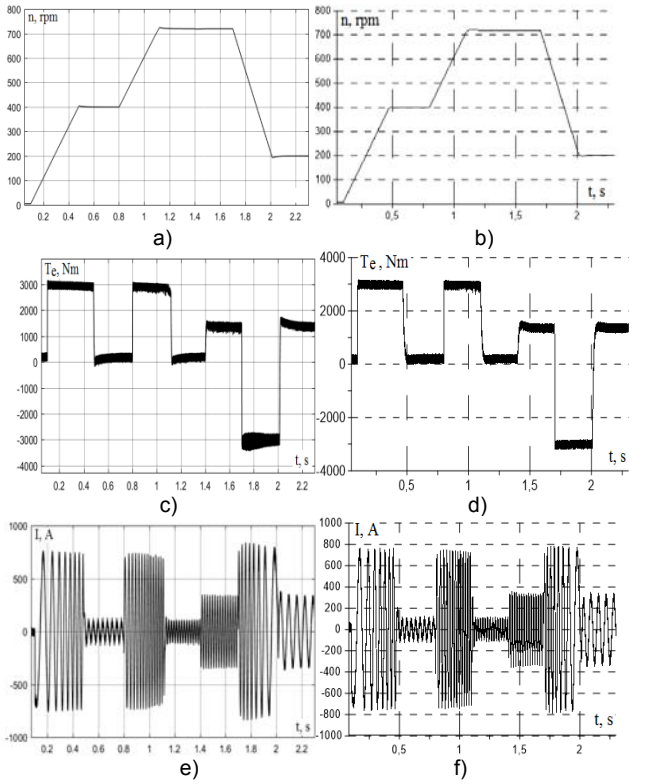

Fig. 5. Rotation speed (a, b), electromagnetic moment (c, d), the stator current (e, f): a, c, e – the calculations by Matlab/Simulink model, b, d, f – the calculations by the developed model.

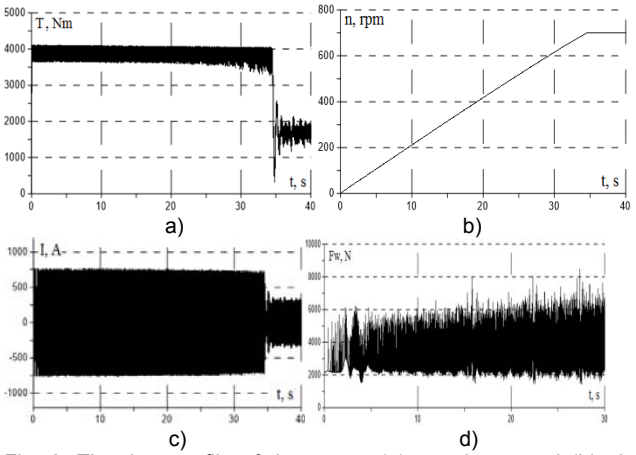

Fig. 6. The time profile of the torque (a), rotation speed (b), the stator current (c), the force that acts on the wheel $F_w = T_w/r_w$ (r_w - radius of the wheel) (d), calculated for the maximum acceleration mode.

Conclusion

The mathematical model of the asynchronous electric drive with DTC, which was designed using the method of the average voltages on the numeric integration step, demonstrated an advanced operational performance. It performs real-time continuous calculations during a long time (up to 12 h) for the observer and controller modelling and synthesizing. The designed model can be used in the hybrid systems, which combine the computer models of the AC e-motor and physical e-motors of several locomotion modules.

This study has been supported by a grant of the NATO Science for Peace and Security Programme: MYP SPS G5167 "Agile Tyre Mobility for Severe Terrain Environments".

Authors

Prof. DSc. Andriy Kutsyk, Lviv Polytechnic National University, Institute of Power Engineering and Control Systems, Bandera str., 79013 Lviv, Ukraine; UTP University of Science and Technology in Bydgoszcz, Institute of Electrical Engineering, al. prof. S. Kaliskiego 7, 85-796 Bydgoszcz; E-mail: andrii.s.kutsyk@lpnu.ua. Prof. DSc. Andriy Lozynskyy, Lviv Polytechnic National University, Institute of Power Engineering and Control Systems, Bandera str., 79013 Lviv, Ukraine, andriy.o.lozynskyy@lpnu.ua. Prof. DSc. Vladimir Vantsevitch, University of Alabama at Birmingham, Department of Mechanical Engineering, Business & Engineering Complex Room 257, 1150 10th Avenue South Birmingham, AL 35294, E-mail: vantsevi@uab.edu. Prof. DSc. Omelian PLAKHTYNA, Lviv Polytechnic National University, Institute of Power Engineering and Control Systems, Bandera str., 79013 Lviv, Ukraine; UTP University of Science and Technology in Bydgoszcz, Institute of Electrical Engineering, al. prof. S. Kaliskiego 7, 85-796 Bydgoszcz; E-mail: plakht@utp.edu.pl. Prof. DSc. Lyubomyr DEMKIV, Lviv Polytechnic National University, Institute of Computer Science and Information Technologies, Bandera str., 79013 Lviv, Ukraine, E-mail: demkivl@gmail.com.

REFERENCES

[1] BÉLANGER, J., P. VENNE, and J.-N. PAQUIN, The what, where, and why of real-time simulation. *Planet RT 1 (1)*, 2010, pp. 37-49. Available at: https://www.opal-rt.com/wp-content/themes/enfold-opal/pdf/L00161_0436.pdf

[2] FANG, K., Y. ZHOU, P. MA and M. YANG, Credibility evaluation of hardware-in-the-loop simulation systems. In: *2018 Chinese Control And Decision Conference (CCDC)*. Shenyang, 2018, pp. 3794-3799. DOI: 10.1109/CCDC.2018.8407782.

[3] VILSEN, S. A., M. F∅RE and A. J. S∅RENSEN. Numerical models in real-time hybrid model testing of slender marine systems. In: *OCEANS 2017 – Anchorage*. Anchorage, AK, 2017, pp. 1-6.

[4] PROKHOROV, A., Yu. BOROVIKOV, and A. GUSEV. Real time hybrid simulation of electrical power systems: Concept, tools, field experience and smart grid challenges. In: *Int. J. Smart Grid Clean Energy*, vol. 1, no. 1, Sep. 2012, pp. 67–68.

[5] BOROVIKOV, Y.S., A.O. SULAYMANOV, A.S. GUSEV and M.V. ANDREEV. Simulation of automatic exciting regulators of synchronous generators in hybrid real-time power system simulator. In: *2nd Intern. Conference "Systems and Informatics (ICSAI)*, Shanghai, 2014, pp. 153 – 158.

[6] Plakhtyna, O., Kutsyk, A., Semeniuk, M. An analysis of fault modes in an electrical power-generation system on a real-time simulator with a real automatic excitation controller of a synchronous generator. *Elektrotehniski Vestnik/Electrotechnical Review,* 2019, 86(3), pp. 104-109.

[7] LIU J., L. ZHANG, Q. CHEN, S. QUAN and R. LONG. Hardware-in-the-loop test bench for vehicle ACC system. In: *2017 Chinese Automation Congress (CAC)*, Jinan, 2017, pp. 1006-1011.

[8] XING J. and H. HE. The application of hardware-in-the-loop on the hybrid power system's simulation. In: *2008 IEEE Vehicle Power and Propulsion Conference*, Harbin, 2008, pp. 1-4.

[9] IACCHETTI, M. F., R. PERINI, M. S. CARMELI, F. CASTELLI-DEZZA and N. BRESSAN. Numerical Integration of ODEs in Real-Time Systems Like State Observers: Stability Aspects. *IEEE Transactions on Industry Applications*. Jan.-Feb. 2012, vol. 48, no. 1, pp. 132-141.

[10] Plakhtyna, O., Kutsyk, A., Lozynskyy, A. Method of average voltages in integration step: Theory and application. *Electrical Engineering,* 2020, 102(4), pp. 2413-2422.

[11] AMMAR A. *et al*. Predictive direct torque control with reduced ripples and fuzzy logic speed controller for induction motor drive. In: *2017 5th International Conference on Electrical Engineering - Boumerdes (ICEE-B)*, Boumerdes, 2017, pp. 1-6. doi: 10.1109/ICEE-B.2017.8191978

[12] AMMAR, A., A. BOUREK and A. BENAKCHA. Efficiency optimization for sensorless induction motor controlled by MRAS based hybrid FOC-DTC strategy. In: *2017 International Conference on Control, Automation and Diagnosis (ICCAD)*, Hammamet, 2017, pp. 152-157. doi: 10.1109/CADIAG.2017.8075648.

[13] KRIM, S., S. GDAIM, A. MTIBAA and M. F. MIMOUNI. Real time implementation of DTC based on sliding mode speed controller of an induction motor. In: *2015 16th International Conference on Sciences and Techniques of Automatic Control and Computer Engineering (STA)*, Monastir, 2015, pp. 94-100. doi: 10.1109/STA.2015.7505139.

[14] VANTSEVICH, V.V., A. LOZYNSKYY, L. DEMKIV, I. HOLOVACH. Fuzzy Logic Control of Agile Dynamics of a Wheel Locomotion Module. In: *IAVSD International Symposium on Vehicle Dynamics*, Rockhampton, Australia, August 14-18, 2017, pp 401-404.

[15] ZHANG, L, G. WEI and D. XIAOLIN. Real-time ground dynamics simulation method of a wheeled mobile robot in virtual terrain. In: *2012 International Conference on Computer Science and Information Processing (CSIP)*, Xi'an, Shaanxi, 2012, pp. 355-358. DOI: 10.1109/CSIP.2012.6308867

[16] MONGA, M., M. KARKEE, S. SUN, L. K. TONDEHAL, B. STEWARD, A. KELKAR and J. ZAMBRENO. Real-time Simulation of Dynamic Vehicle Models using a High-performance Reconfigurable Platform, *Procedia Computer Science*. 2012, Volume 9, pp. 338-347. DOI:10.1016/j.procs.2012.04.036.

[17] MA, Z., Z. LIU, J. LU and H. CHEN. Study on Real-Time Simulation System of Vehicle Dynamics Via ve-DYNA. In: *2006 IEEE International Conference on Vehicular Electronics and Safety*, Beijing, 2006, pp. 454-458. DOI: 10.1109/ICVES.2006.371634

[18] PLAKHTYNA O. *The mathematical modeling of the electrotechnical systems with semiconductor converters*. Lviv: Vushcha shkola, 1986. 164 p.(in Russian)

[19] PŁACHTYNA, O., Z. KŁOSOWSKI, R. ŻARNOWSKI. Mathematical model of DC drive based on a step-averaged voltage numerical method. *Przegląd Elektrotechniczny*. 2011, 87, 12a, pp.51-56. (in Polish).

[20] PŁACHTYNA, O., Z. KŁOSOWSKI, R. ŻARNOWSKI. Efficiency evaluation of average-step voltages method comparing to clasical methods of numerical integration applied to mathematical models of eletrical circuits. *Prace Naukowe Politechniki Śląskiej. Elektryka*. 2012, 217, 1, pp.121-133. (in Polish).

[21] KUTSYK, A.S. The object-oriented method for analize of electromechanical systems". *Technical electrodynamics.* 2006, №.2, pp. 57–63. (in Ukrainian).

[22] VANTSEVICH, V. Agile Dynamics Fundamentals for Tire Slippage Modeling and Control. In: *ASME DETC2014-34464*, August 17-20, Buffalo, NY, 2014. doi:10.1115/DETC2014-34464

[23] VANTSEVICH, V. V., A. LOZYNSKYY, L. DEMKIV. A Wheel Rotational Velocity Control Strategy for An open-Link Locomotion Module. In: *19th International and 14th European-African Regional Conference of the ISTVS*, Budapest, Hungary, September 25-27, 2017, pp. 151-162

[24] VANTSEVICH, V. V., J. GRAY, J. PALDAN. An agile tire slippage estimation based on new tire and wheel rolling characteristics. In: *13th European Conference of the ISTVS*, Rome, Italy, 2015